Available online at www.sciencedirect.com

SciVerse ScienceDirect

Ceramics International 39 (2013) 4213–4219

CERAMICS INTERNATIONAL

www.elsevier.com/locate/ceramint

Influence of milling time on the synthesis, microstructure and mechanical properties of ZrB_2–SiC–ZrO_{2f} ceramic composites

Jia Lin*, Xinghong Zhang, Wenbo Han, Di Sun

National Key Laboratory of Science and Technology on Advanced Composites in Special Environments, Harbin Institute of Technology, Harbin 150001, PR China

Received 12 October 2012; accepted 2 November 2012
Available online 8 November 2012

Abstract

Zirconium diboride toughened by silicon carbide and zirconia fiber (ZrB_2–SiC–ZrO_{2f}) was prepared by using planetary ball mill and the effect of milling time was investigated. The results showed that both the length of fiber and particle size of ZrB_2–SiC-matrix were reduced as the ball milling time increased. When milling time varied from 8 h to 12 h, the accumulated fibers and agglomerated particles were observed. The production of a homogeneous ceramic could be successfully achieved by using a combination of 20 h milling time and hot-pressing at 1850 °C for 60 min under a uniaxial load of 30 MPa. The optimal flexural strength and fracture toughness of the hot-pressed ZrB_2–SiC–ZrO_{2f} ceramics reached 1084 MPa and 6.8 MPa $m^{1/2}$, respectively. The main toughening mechanisms were fiber debonding, fiber pull-out and transformation toughening. The results indicated that the ball milling technique was proposed as a potential and simple method to obtain usable quantities of ZrB_2–SiC–ZrO_{2f} ceramic.

Keywords: A. Hot pressing; A. Milling; B. Composites; B. Fibers

1. Introduction

Because of the unique properties of Zirconium diboride (ZrB_2) based ultra-high temperature ceramics (UHTC), such as high melting point (> 3000 °C), high thermal and electrical conductivities, chemical inertness against molten metals, and great thermal shock resistance [1–3], it is a potential material for high-temperature structural application, including furnace elements, hypersonic aircraft, plasma-arc electrodes, reusable launch vehicles, or rocket engines and thermal protection structures for leading edge parts on hypersonic reentry space vehicles at over 1800 °C [4,5]. However, monolithic ZrB_2 ceramic is difficult to get densified due to the strong covalent bonding and low self-diffusion of Zr and B [6,7]. Besides, the intrinsic brittleness is another obstacle for ZrB_2 ceramic to be used widely, especially for applications in severe environment [8]. In our previous research, it has been indicated that ZrB_2 toughened by silicon carbide particle (SiC_p) and zirconia fiber (ZrO_{2f}) exhibits more excellent properties than that of either individual component [9,10].

As one of the special family of ceramic fibers, stabilized polycrystalline ZrO_2 fiber exhibits high strength from 1.5 to 2.6 GPa, which attributes to the absorption of fracture energy caused by the stress-induced martensitic phase transformation toughening of ZrO_2 from tetragonal (t-ZrO_2) to monoclinic phase (m-ZrO_2) in the stress field of propagating cracks [11,12]. Because of high melting point and mechanical properties, ZrO_2 fiber has been widely applied as the reinforcement of metals, plastics, ceramics and high temperature insulating materials [13,14]. Obviously, it is advantageous to couple the fiber toughening and transformation toughening together in order to improve the toughness of matrix material.

Ball milling is a universal raw material preparation involving cold welding and fracturing of powder particles, and it is viable for large-scale production as well as convenient [15]. Aim to obtain the appropriate particle

*Correspondence to: Center for Composite Materials, Harbin Institute of Technology, Room 101, Building A Science Park of HIT No. 2 Yi-Kuang Street, Nan-Gang District, Harbin 150080, China.
Tel./fax: +86 451 8640 2382.
E-mail address: jiajia10182003@hit.edu.cn (J. Lin).

0272-8842/$ - see front matter © 2012 Elsevier Ltd and Techna Group S.r.l. All rights reserved.
http://dx.doi.org/10.1016/j.ceramint.2012.11.003

size, required phase and structure of the final product, it is necessary to optimize the parameters in the ball milling process, such as milling machine, milling speed, milling time, charge ratio, chemical composition of the powder mixture, temperature nature of milling atmosphere, etc. [16] Above all parameters, milling time is one of the most important variables to be studied. With increasing the ball milling time, the particle size of raw powder is decreased, the specific surface area and surface reactivity are increased, so as to lower sintering temperature and accelerate the sintering. But too long milling time will lead to excessive heating of the vessel, lower powder yields and increase wear of milling medium causing increased contamination [17,18]. Moreover, ZrO_2 fiber is chosen as reinforcement in the present work, and the collision and extrusion between grinding balls will cause fiber breakage. So it is important to investigate the effect of milling process on the microstructure of fibers.

The previous work proved that ZrB_2 added with 20 vol% SiC and 15 vol% ZrO_{2f} (ZSZ) had good comprehensive properties [9]. On these bases, the effect of milling time on the powder morphology, particle size, phase structure and phase formation of ZSZ ceramics were investigated. The milling parameters were optimized to coordinate with milling time. The purpose of this work was to find the most suitable milling time for the ZSZ ceramics.

2. Experimental procedures

Commercially available ZrB_2 powder (2 μm, purity > 99.5%, Northwest Institute for non-ferrous metal research, China), SiC (1 μm, purity > 99.5%, Weifang Kaihua Micropowder Co., Ltd., China.) and ZrO_2 fiber (Mean diameter and length are 5–8 μm and 200 μm, respectively, purity > 99%, Shandong Huolong Ceramic Fiber Co., Ltd., China) were used as raw materials. The powders were weighed in proportion to the stoichiometric ratio to yield ZrB_2–20 vol% SiC_p–15 vol%ZrO_{2f} and then homogeneously mixed in a polyethylene bottle using zirconia balls and ethanol as the grinding media. Ball milling was performed using a QM-1SP4 planetary ball mill at a rotation speed of 220 rpm. A ball to powder weight ratio of 10:1 was selected to ensure high efficiency. Different ball milling times were used: 8 h, 10 h, 12 h, 16 h, 20 h and 24 h (Table 1). The resulting powder mixtures were hot-pressed at 1850 °C for 60 min under a uniaxial load of 30 MPa in Ar atmosphere.

The phase composition was determined by X-ray diffraction (XRD; Rigaku, Dmax-rb, CuKa = 1.5418 Å). According to the formula of Toraya et al. [19], the volume fraction of the m-ZrO_2 (V_m) was calculated by measuring the intensities of (111) and (111(_)) reflections of the monoclinic phase and the (111) peak of the tetragonal phase:

$$V_m = \frac{1.311X_m}{1+0.311X_m} \tag{1}$$

$$X_m = \frac{I_m(111)+I_m(11\overline{1})}{I_m(111)+I_m(11\overline{1})+I_t(111)} \tag{2}$$

where, X_m denotes the integrated intensity ratio, I_m and I_t are the peak intensities of the m-ZrO_2 and t-ZrO_2, respectively. Furthermore, the obtained V_m was individually normalized to the volume fraction of ZrO_2 (V_{ZrO_2}) in each composite as follows:

$$V_{mtot} = V_m \times V_{ZrO_2} \times 100\% \tag{3}$$

Therefore, the result of V_{mtot} on the fracture surface minus the one on the polished surface equaled to the transformation fraction from t-ZrO_2 to m-ZrO_2 during fracture (i.e., t-ZrO_2 transformability).

The bulk density of the specimens was measured by the Archimedes method. The microstructural features and fragmented surfaces of the hot-pressing composite were observed by scanning electron microscopy (SEM, FEI Sirion, Holland) with simultaneous chemical analysis by energy dispersive spectroscopy (EDS, EDAX Inc). Flexural strength (σ) was tested in three point bending on 3 mm by 4 mm by 36 mm bars, using a 30 mm span and a crosshead speed of 0.5 mm min^{-1}. Each specimen was ground and polished with diamond slurries down to a 1 μm finish. The edges of all the specimens were chamfered to minimize the effect of stress concentration due to machining flaws. Fracture toughness (K_{IC}) was evaluated by a single-edge notched beam test with a 16 mm span and a crosshead speed of 0.05 mm min^{-1} using 2 mm by 4 mm by 22 mm test bars, on the same jig used for the flexural strength. All flexural and fracture bars were cut with the tensile surface perpendicular to the hot-pressing direction. A minimum number of six specimens were tested for each experimental condition.

Table 1
Materials and relative densities of sintered composites.

Samples	Milling time (h)	Sintering condition			Density (g cm^{-3})	Relative density (%)
		Temperature (°C)	Pressure (MPa)	Time (min)		
ZS_pZ_f8	8	1850	30	60	5.35	97.0
ZS_pZ_f10	10	1850	30	60	5.38	97.4
ZS_pZ_f12	12	1850	30	60	5.46	98.9
ZS_pZ_f16	16	1850	30	60	5.44	98.6
ZS_pZ_f20	20	1850	30	60	5.45	98.8
ZS_pZ_f24	24	1850	30	60	5.34	96.7

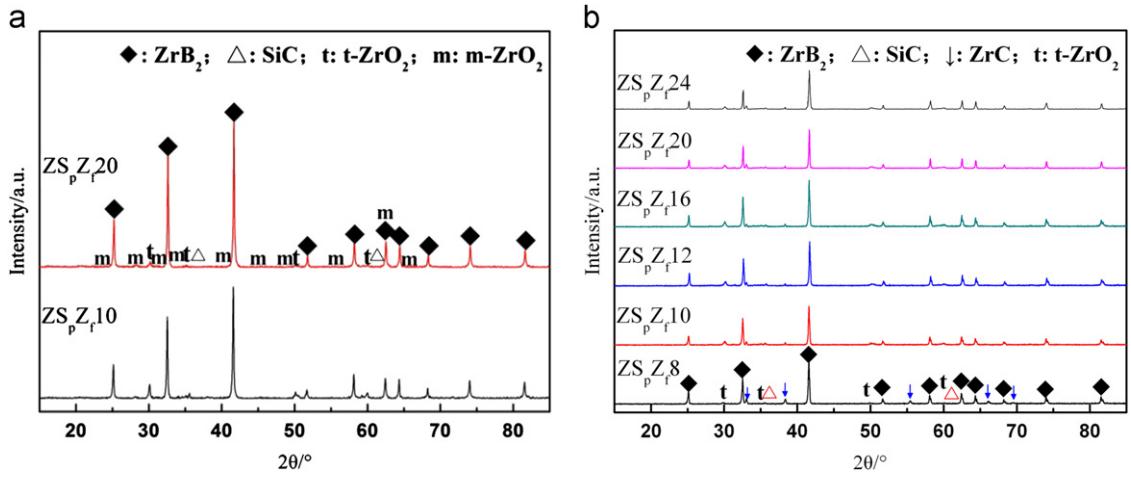

Fig. 1. Typical XRD spectra of (a) ZSZ mixed powders and (b) the polished surfaces of sintered ZSZ ceramics with different milling times.

3. Results and discussions

The XRD spectra of ZBZ mixed powders are shown in Fig. 1a. Phase analysis confirmed that for unsintered powders the main phases were ZrB_2, SiC, *t*-ZrO_2 and minor *m*-ZrO_2. With increasing milling time, the initially sharp diffraction peaks got wider and the absolute intensity decreased. This was due to powder crystallite size refinement and internal strain increase which was induced by the mechanical treatment. However, as shown in Fig. 1b, there appeared a trace of ZrC on the polished surfaces of sintered ZSZ ceramics after hot-pressing, which was attributed to the reaction of SiC with ZrO_2 [9]. And no *m*-ZrO_2 could be detected (Fig. 1b), which indicated that *m*-ZrO_2 had sintered to *t*-ZrO_2 at 1850 °C. Theoretically, if more *t*-ZrO_2 transformed to *m*-ZrO_2 during fracturing process, the transformation toughening will be enhanced.

Fig. 2a–f shows scanning electron micrograph of the ZSZ powders with different milling times. Combined with the inserted analysis of EDS, the rod-like phase was ZrO_2 fiber in Fig. 2 a–f. When milling time was 8 h, the length of fibers changed from ~20 μm to ~100 μm. Meanwhile, the aggregation of some fibers appeared. At this stage of milling, fibers were reduced in different degree by shear and friction between the grinding media, the predominant mechanism in this stage was plastic deformation and fracture. With increasing milling time to 12 h, fracturing and welding became a significant process since the ability of the fibers and matrix particles to accept further plastic deformation was diminished, which led to a progressive reduction of the fiber length and particle size resulting in an increase of the specific surface area. At this stage, the length of fibers was finally equal to the other, but along with the intensification of agglomeration. With further milling to 20 h, the fiber length remained unchanged basically (~20 μm). Moreover, the agglomerated particles were subjected to continuous fragmentation to form finer particles and the accumulation of fibers was scattered by mechanical force with uniform distribution in the matrix. But when milling time was increased to 24 h, fibers were almost broken into particles, which was supposed to have poor fracture toughness and is discussed later.

Fig. 3a–f shows SEM micrographs of the fractured surface of specimens for testing fracture toughness. On the fractured surface, some short fibers fractured were detected when milling time was short (from 8 h to12 h). This was due to the random distribution pattern which made fibers lapped with each other. With increasing milling time (from 16 h to 20 h), it could be seen that fibers were well distributed in ZrB_2 matrix. On the other hand, the fracture surface was rough, which was attributed to the effects of fiber debonding and pull-out. As known, the fracture toughness was related to the fracture model. The fracture model here was mixed in a inter/trans-granular mode which would lead to a higher fracture toughness. As shown in Fig. 3f, when milling time was increased to 24 h, no fibers were found on the fractured surface so that fiber toughening mechanism had no effect.

The ZrB_2 grain sizes of ZSZ ceramics with different milling times are plotted in Fig. 4a, which are determined from SEM images of the fractured surface using an image analysis software package and estimated by measuring at least 120 grains. The size of ZrB_2 grains decreased gradually with increasing milling time and tended to be stable after milling for 20 h, since welding and fracture mechanisms reached equilibrium. According to the classical Hall–Petch relationship given by the formula $\sigma = \sigma_0 + kd^{-1/2}$($\sigma$ is the strength of materials, σ_0 is the strength of materials without any defect, k is material constants, d is grain size), the grain size related with the mechanical properties.

In order to understand the transformation toughening mechanisms of ZrO_{2f}, Fig. 4b shows the calculated results according to Eqs. (1) and (2). The trend of development of *t*-ZrO_2 transformability was consistent with the change of mechanical properties. The dispersion of fibers in the

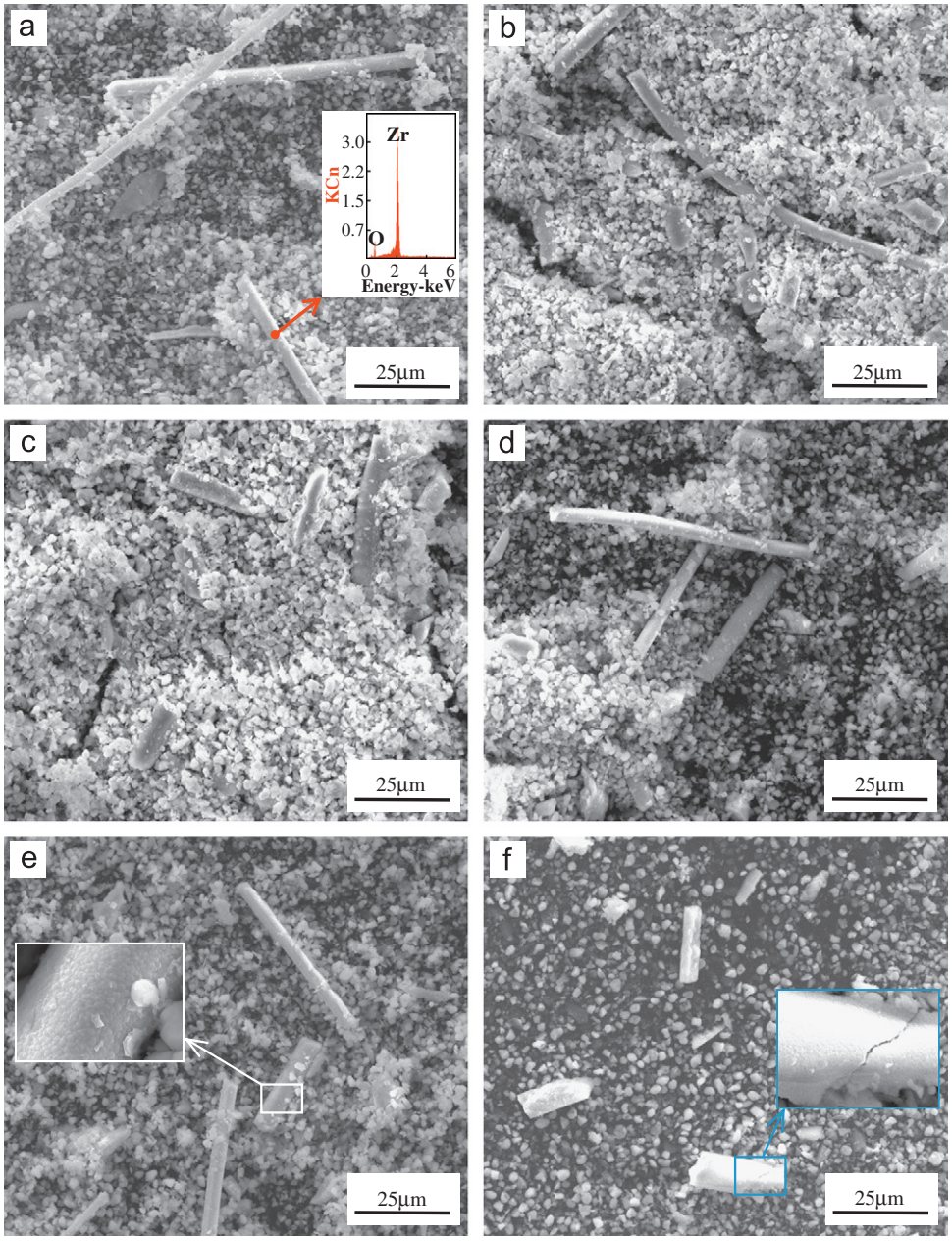

Fig. 2. SEM micrographs of the polished surface of ZSZ ceramics with different milling times: (a) ZS_pZ_f8 (b) ZS_pZ_f10 (c) ZS_pZ_f12 (d) ZS_pZ_f16 (e) ZS_pZ_f20 and (f) ZS_pZ_f24.

matrix was quite homogeneous, which was favorable to load-sharing under a testing load and could promote the t-ZrO_2 to m-ZrO_2 transformation. According to previous study [21,22], when subjected to the external load, stress concentration in the ceramic would bring the phase transformation from t-ZrO_2 to m-ZrO_2 with the volume expansion (4–5%), which would hinder the crack growing or propagating and exhaust the fracture energy. If more t-ZrO_2 transforms to m-ZrO_2 during fracture, the transformation toughening would be increased.

Fig. 5 shows the flexural strength and fracture toughness of ZSZ ceramics with different milling times. It is well known that strength decreases exponentially as the porosity increases for ceramic materials [20]. When a combination of density measurements (Table 1) and SEM analysis was used, no obvious pores were found (relative density $>96\%$), so the effect of porosity could be ignored. Results exhibited some fluxion undulation that the flexural strength and fracture toughness decreased with the increase of milling time till 12 h, then increased with the further increase of milling time until 20 h, and at last decreased as the milling time was 24 h, which was consistent with the analysis of the SEM microstructure. The strength of the ceramics is a combination of matrix strength, reinforcement strength, interface strength and the residual stress induced by thermal expansion mismatch. Obviously, the accumulated fibers and agglomerated particles

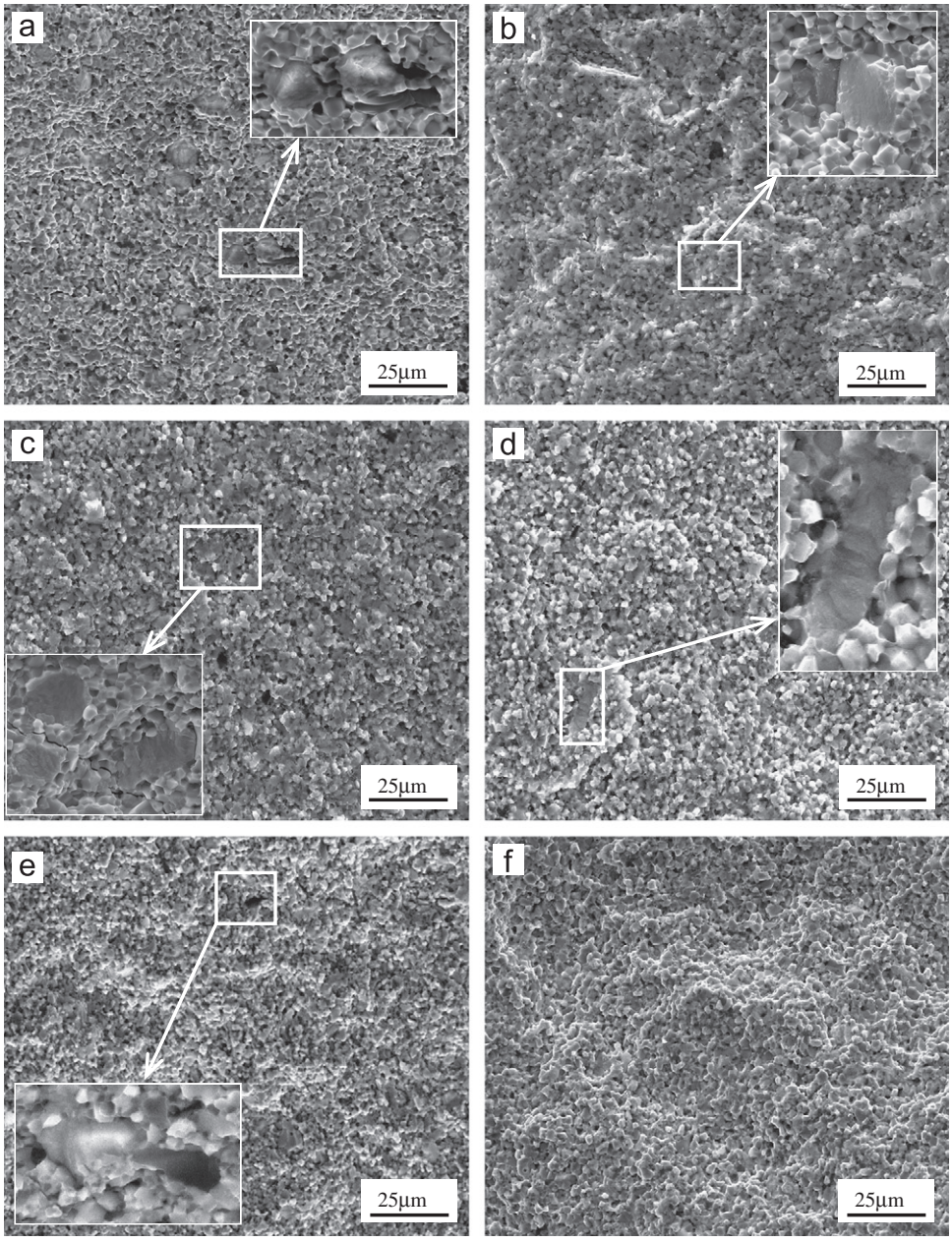

Fig. 3. SEM micrographs of the fractured surface of ZSZ ceramics with different milling times: (a) ZS_pZ_f8 (b) ZS_pZ_f10 (c) ZS_pZ_f12 (d) ZS_pZ_f16 (e) ZS_pZ_f20 and (f) ZS_pZ_f24.

are not beneficial to the fiber debonding and pull-out, which would reduce the mechanical properties. The optimal milling time was 20 h, and the flexural strength and fracture toughness could reach 1084 MPa and 6.8 MPa $m^{1/2}$, respectively.

4. Conclusions

The effect of milling time on the synthesis of ZrB_2 added with 20 vol% SiC and 15 vol% ZrO_{2f} was investigated by using a wet mechanical balling technique carried out in a planetary ball mill. The resulting powders had a range of fiber length and particle size, depending on milling times. When the milling time was shorter than 12 h, the accumulated fibers and agglomerated particles were observed. On the other hand, when the milling time was too much such as 24 h, the fibers were broken to particles, which was also harmful for improving the mechanical properties. The optimal production of a homogeneous ceramic could be successfully achieved by using a combination of 20 h milling time and hot-pressing at 1850 °C for 60 min under a uniaxial load of 30 MPa. The flexural strength and fracture toughness reached 1084 MPa and 6.8 MPa $m^{1/2}$, respectively. The toughening mechanisms were fiber debonding, fiber pull-out and transformation toughening. The potential of ball milling technique was proposed as a

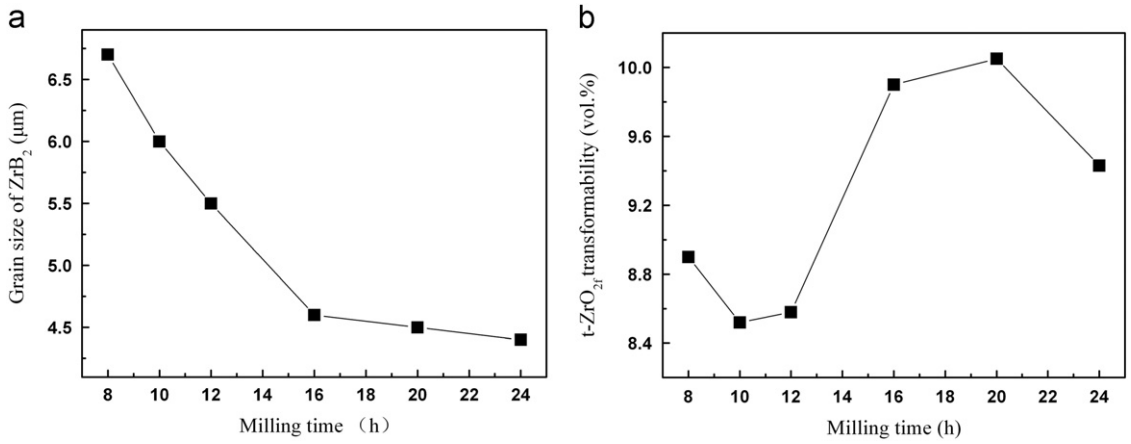

Fig. 4. ZrB_2 Grain size (a) and *t*-ZrO_2 transformability during fracture (b) for ZSZ ceramics with different milling times.

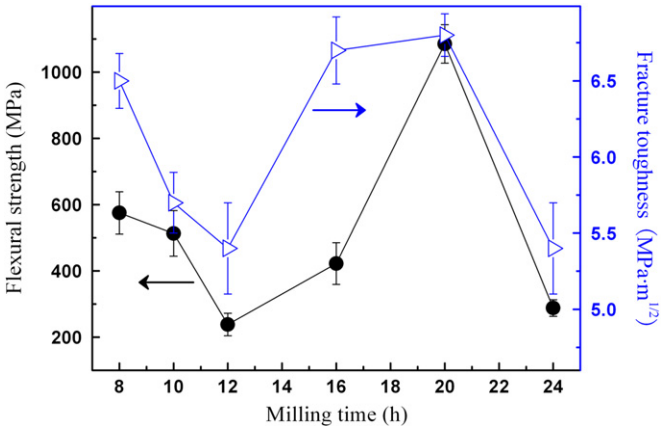

Fig. 5. Flexural strength and fracture toughness of ZSZ ceramics with different milling times.

simple method to obtain usable quantities of ZrB_2–SiC–ZrO_{2f} ceramic.

Acknowledgments

This work was supported by the NSFC (51072042, 10725207) and the Science Fund for Outstanding Youths of Heilongjiang Province.

References

[1] Z.H. Lü, D.L. Jiang, J.X. Zhang, Q.L. Lin, Processing and properties of ZrB_2–SiC composites obtained by aqueous tape casting and hot pressing, Ceramics International 37 (2011) 293–301.
[2] Y. Champion, S. Hagege, M. Masse, Structural analysis of phases and heterophase interfaces in the zirconium–boron system, Journal of Materials Science 33 (1998) 4035–4041.
[3] Y.B. Lee, H.C. Park, K.D. OH, C.R. Bowen, R. Stevens, Self-propagating high-temperature synthesis of ZrB_2 in the system ZrO_2–B_2O_3–Fe_2O_3–Al, Journal of Materials Science Letters 19 (2000) 469–471.
[4] M. Singh, R. Asthana, Joining and integration of ZrB_2-based ultra-high temperature ceramic composites using advanced brazing technology, Journal of Materials Science 45 (2010) 4308–4320.
[5] R. Lingappa, D. Canchi, J. Vikram, Fabrication and mechanisms of densification of ZrB_2-based ultra high temperature ceramics by reactive hot pressing, Journal of the European Ceramic Society 30 (2010) 129–138.
[6] S.B. Zhou, Z. Wang, W. Zhang, Effect of graphite flake orientation on microstructure and mechanical properties of ZrB_2–SiC–graphite composite, Journal of Alloys and Compounds 485 (2009) 181–185.
[7] W.Z. James, E.H. Greg, G.F. William, Thermal shock resistance of ZrB_2 and ZrB_2–30% SiC, Materials Chemistry and Physics 112 (2008) 140–145.
[8] Y.G. Wang, M. Zhu, L.F. Cheng, L.T. Zhang, Fabrication of SiC_w reinforced ZrB_2-based ceramics, Ceramics International 36 (2010) 1787–1790.
[9] J. Lin, X.H. Zhang, Z. Wang, W.B. Han, Microstructure and mechanical properties of ZrB_2–SiC–ZrO_{2f} ceramic, Scripta Materialia 64 (2011) 872–875.
[10] J. Lin, X.H. Zhang, Z. Wang, W.B. Han, H. Jin, Microstructure and mechanical properties of hot-pressed ZrB_2–SiC–ZrO_{2f} ceramics with different sintering temperatures, Materials and Design 34 (2012) 853–856.
[11] Y. Toshinobu, Synthesis of polycrystalline zirconia fibre with organozirconium precursor, Journal of Materials Science 25 (1990) 2394–2398.
[12] S.D. Yuh, Y.C. Lai, C.C. Chou, H.Y. Lee, $YNbO_4$-addition on the fracture toughness of ZrO_2(3Y) ceramics, Journal of Materials Science 36 (2001) 2303–2311.
[13] P.K. Chakrabarty, M. Chatterjee, M.K. Naskar, B. Siladitya, D. Ganguli, Zirconia fibre mats prepared by a sol-gel spinning technique, Journal of the European Ceramic Society 21 (2001) 355–361.
[14] A. Yoshimoto, K. Takahiro, T. Hiroshi, G. Takahiro, N. Yukinori, M. Takahisa, Preparation of continuous zirconia fibres from polyzirconoxane synthesized by the facile one-pot reaction, Journal of Materials Science 33 (1998) 1863–1870.
[15] H.B. Feng, D.C. Jia, Y. Zhou, Influence factors of ball milling process on BE powder for reaction sintering of TiB/Ti–4.0Fe–7.3Mo composite, Journal of Materials Processing and Technology 182 (2007) 79–83.
[16] M.C. Musa, O. Sadan, C. Abdullah, F. Tezer, Effect of milling time on the synthesis of magnetite nanoparticles by wet milling, Materials Science and Engineering B 172 (2010) 72–75.
[17] M.O. Lai, L. Lu, W. Laing, Formation of magnesium nanocomposite via mechanical milling, Composite Structures 66 (2004) 301–304.

[18] A.H. Stephen, A.K. Kevin, Effects of ball milling time on the synthesis and consolidation of nanostructured WC–Co composites, International Journal of Refractory Metals and Hard Materials 27 (2009) 937–948.

[19] H. Toraya, M. Yoshimura, S. Somiya, Calibration curve for quantitative analysis of the monoclinic–tetragonal ZrO_2 system by X-ray diffraction, Communications of the American Ceramic Society 67 (1984) 119–121.

[20] B. Dusan, M. Branko, B. Snezana, Z. Slavica, K. Vladimir, Pressureless sintering of internally synthesized SiC–TiB_2 composites with improved fracture strength, Journal of Alloys and Compounds 509 (2011) 990–996.

[21] C.L. Yang, H.I. Hsiang, C.C. Chen, Characteristics of yttria stabilized tetragonal zirconia powder used in optical fiber connector ferrule, Ceramics International 31 (2005) 297–303.

[22] D.J. Chen, W.J. Li, X.H. Zhang, P. Hu, J.C. Han, C.Q. Hong, W.B. Han, Microstructural feature and thermal shock behavior of hot-pressed ZrB_2–SiC–ZrO_2 composite, Materials Chemistry and Physics 116 (2009) 348–352.